

# Synthesis of MoS<sub>2</sub> Nanoarray Materials and Electrocatalytic Performance for Hydrogen Evolution over a Wide pH Range

Shi Zhang, Danya Lv, Lei Zhang

Wuhu Institute of Technology, Wuhu, Anhui, China

**Abstract:** With the excessive use of fossil energy, the global energy crisis and environmental pollution are becoming increasingly serious, which forces the international community to develop environmentally friendly and sustainable new energy sources. Hydrogen energy has attracted widespread attention due to its many advantages such as high efficiency and no secondary pollution. Water electrolysis technology is considered to be one of the most ideal ways to produce green hydrogen. As an electrocatalyst for hydrogen evolution, MoS<sub>2</sub> has attracted the attention of researchers due to its good conductivity. In this paper, MoS<sub>2</sub> nanosheet arrays (MoS<sub>2</sub>@Mo) were synthesized on the surface of molybdenum foil in a controlled manner by a one-step liquid-phase synthesis method. The lamellar nanosheet array structure significantly improved the packing phenomenon of MoS<sub>2</sub> nanosheets. This exposes more catalytically active sites at the edge of the MoS<sub>2</sub> lamellar and increases the contact area between the material and the electrolyte. Due to the good electrical conductivity of molybdenum foil, as well as its acid and alkaline resistance, MoS<sub>2</sub> nanosheet array materials are directly grown on the surface of molybdenum foil, which not only improves the electron transfer during the hydrogen evolution reaction, but also can be directly used as electrodes to catalyze hydrogen evolution reactions in acidic and alkaline environments. The electrochemical hydrogen evolution performance test shows that the synthesized MoS<sub>2</sub>@Mo material has good catalytic activity and stability under both acidic and alkaline conditions, and the overpotentials of 142.5 mV and 40 mV are required when the current density reaches 10 mA.cm<sup>-2</sup>, respectively.

**Keywords:** Electrocatalysis; Hydrogen evolution reaction; MoS<sub>2</sub>

## 1. Introduction

At present, the widespread use of fossil fuels not only causes a growing environmental problem, but also faces the problem of energy depletion. Hydrogen is considered one of the ideal green energy sources to replace fossil fuels due to its high energy density and clean combustion products<sup>[1]</sup>. Electrochemical water splitting technology uses renewable energy sources such as solar, hydro, wind, and tidal energy to provide an environmentally friendly and sustainable technology for the large-scale production of high-purity hydrogen<sup>[2]</sup>. However, due to the large catalytic hydrogen evolution reaction (HER) overpotential in the process of electrochemical water splitting, the energy consumption is high and the hydrogen production efficiency is low, which hinders the practical application of electrochemical water splitting to hydrogen production. Therefore, a highly active and stable HER catalyst is required<sup>[3]</sup>. Currently, precious metals such as Pt are the best catalysts for HER. However, their scarcity and high cost hinder their large-scale practical application. Therefore, there is a need to design and manufacture abundant HER electrocatalysts.

Two-dimensional (2D) transition metal chalcogenide compounds with layered structure have been identified as suitable HER catalysts due to their low cost and low hydrogen adsorption Gibbs free energy, such as MoS<sub>2</sub><sup>[4][5]</sup>. Both theoretical calculations and experimental results show that the catalytically active site of HER is located at the edge of the MoS<sub>2</sub> layer<sup>[6][7]</sup>. Therefore, exposing more active edge sites is an effective way to increase their catalytic activity at HER. However, the intrinsic structure of the 2D lamellar structure makes it prone to agglomeration<sup>[8]</sup>, which reduces the number of available edge active sites and impairs HER performance<sup>[7]</sup>. In addition, the inherently poor electron conductivity of MoS<sub>2</sub> also reduces the efficiency of its electrocatalytic hydrogen evolution reaction<sup>[9]</sup>. One of the effective ways to address the above shortcomings is to use highly conductive materials as substrates to form uniformly distributed nanosheet array structures perpendicular to the substrate surface<sup>[10][11][12][13][14][15]</sup>.

Molybdenum foil (Mo) has good electrical conductivity and resistance to acids and alkalis<sup>[16][17][18]</sup>. Therefore, we chose Mo foil as the substrate and used it as the molybdenum source<sup>[19][20]</sup> to grow homogeneous and well-dispersed MoS<sub>2</sub> nanosheet arrays directly in situ on the surface of molybdenum foil through a simple one-step liquid-phase synthesis route. The prepared MoS<sub>2</sub> nanosheet array@molybdenum foil (MoS<sub>2</sub>@Mo) material can be directly used as an electrode to catalyze HER, and exhibits good HER catalytic activity and stability in both acidic and alkaline environments.

## 2. Experimental part

### 2.1 Main reagents and instruments

The main instruments and reagents used in the experiment are shown in Tables 1 and 2

Table 1: Equipment used in the experiment

Instrument name	Model	Production units
Electronic balances	FA2004N	Shanghai Precision Instrument Co., Ltd
Ultrasonic cleaner	PS-1010SMHT	Hefei Panfeng Ultrasonic Technology Co., Ltd
High-pressure reactor	LC-KH-300	Shanghai Lichen Instrument Technology Co., Ltd
centrifuge	TG16MW	Hunan Hexi Instrument Co., Ltd
Electric blast drying oven	DGT-G70	Hefei Huadeli Scientific Equipment Co., Ltd
Magnetic stirrer	HJ-6	Changzhou Jintan District Baita Xinhong Instrument Factory
Potentiostats	CHI-660E	Shanghai Chenhua Instrument Co., Ltd

Table 2: Reagents used in the experiment

reagent	specification	Production units
Nitric acid(HNO <sub>3</sub> )	AR	Sinopharm Chemical Reagent Co., Ltd
Sulfur(S)	AR	Shanghai Maclean Biochemical Technology Co., Ltd
Ethanol absolute(C <sub>2</sub> H <sub>5</sub> OH)	AR	Sinopharm Chemical Reagent Co., Ltd
HCl	AR	Sinopharm Chemical Reagent Co., Ltd
acetone(CH <sub>3</sub> COCH <sub>3</sub> )	AR	Sinopharm Chemical Reagent Co., Ltd
N <sub>2</sub> H <sub>4</sub> ·H <sub>2</sub> O	AR	Shanghai Aladdin Biochemical Technology Co., Ltd
Mo foil	99.99%	--

### 2.2 Preparation of the product

#### 2.2.1 Substrate pretreatment

The treatment of molybdenum foil is as follows: first, 1cm × 4 cm of molybdenum foil (Mo foil) is cut, sonicated with acetone solution for 10 min to remove the oil stain on the surface, and then sonicated with concentrated hydrochloric acid solution twice for 15 min to remove the oxide on the surface, and then washed with deionized water and ethanol for many times, and put into a blast drying oven (50°C) for drying.

#### 2.2.2 MoS<sub>2</sub>@Mo synthesis of nanomaterials

Different amounts of sulfur powder (S) (0.1 mmol, 0.3 mmol, 0.6 mmol) were weighed and put into 10 mL of water and 20 mL of absolute ethanol and stirred, the stirring temperature was 40 °C, the stirring time was 1 hour, and the solution changed from colorless to light yellow. Then put the washed and dried molybdenum foil into the above solution, and finally add 3 mL N<sub>2</sub>H<sub>4</sub>·H<sub>2</sub>O. The solution was added to the 50 mL PTFE reactor lining, and the PTFE reactor lining was placed into the high-pressure reactor, and finally the reactor was placed in a blast drying oven and reacted at 200 °C for 12 h. After the oven cooled to room temperature, the Mo foil was taken out, washed with deionized water and ethanol several times, and then placed in a blast drying oven and dried at 50 °C for 5 h.

#### 2.2.3 Prepare the working electrode

The dried product was prepared into a working electrode for electrochemical performance test, and 5 mg of the product was weighed and dispersed in a mixture of 10 μL of Nafion, 500 μL of ultrapure water and 500 μL of ethanol solution, and a homogeneous suspension was formed by ultrasonic for 30

min. The glassy carbon electrode was ground and polished with a flannel cloth, and then 5  $\mu\text{L}$  of suspension was evenly dropped on the surface of the glassy carbon electrode (geometric area of 0.196  $\text{cm}^2$ ) with a pipette, and then dried under an infrared lamp. Before the test, the working electrode was placed in 1.0 M KOH solution or 0.5 M  $\text{H}_2\text{SO}_4$  solution to completely wet the electrode surface.

#### Electrochemical testing

Electrochemical performance tests were performed at room temperature, and prior to testing, the electrolyte solution was introduced with  $\text{N}_2$  for 30 minutes to remove the  $\text{O}_2$  contained in the electrolyte solution. The test was performed using a standard three-electrode system, with the carbon rod as the counter electrode, the Ag/AgCl electrode as the reference electrode, and the synthesized  $\text{MoS}_2$  as the working electrode. The electrochemical test requires  $\text{N}_2$  to be introduced all the way and the test is performed in either 1 M KOH (pH = 14) solution or 0.5 M  $\text{H}_2\text{SO}_4$  (pH = 0) solution.

During the test, magnetic stirring is maintained throughout the process to ensure the full transfer of ions in the electrolyte and all potentials

The reversible hydrogen electrode potential (RHE) is used as a reference. All measured potentials were calibrated using the formula  $E(\text{RHE}) = E(\text{Ag}/\text{AgCl}) + 0.197 + 0.0591 \text{ pH}$  compared to the reversible hydrogen electrode (RHE). The test results for LSV are  $iR$ -corrected in this job and have a scan rate of 5 mV/s.

Electrochemical impedance (EIS) can reflect the strength and disadvantage of the charge and mass transfer ability of electrocatalysts during catalytic reactions.

The test conditions for electrochemical impedance are: EIS tests the frequency range of the applied AC signal at a fixed voltage of -0.2 V in the range of 0.01 Hz~1 MHz.

When the CV is tested by cyclic voltammetry, the rotation speed of the rotating rod is 1200 rpm, the scanning rate is 5 mV/s, the test voltage range is 0~0.5 V (vs. Hg/HgO), the CV curves are all corrected by 95%  $iR$ , the electric double layer capacitance (Cdl) is tested by the CV method, and the voltage range of 0.2~0.3 V (vs. Hg/HgO) in the illegal Lady region is tested at 40, 60, 80, 100 and 120 mV/s scanning speeds. The linear relationship between different scanning rates and the corresponding current density is obtained, and the linear slope is calculated to obtain the capacitance value of the electric double layer.

### 3. Results and discussion

#### 3.1 Physical characterization of materials

The synthesized material was characterized. Fig. 1(a) and Fig. 1(d) are scanning electron microscope images (SEM) with 0.1 mmolS added during synthesis, from which it can be seen that a small number of flake  $\text{MoS}_2$  nanosheets grow on the surface of the molybdenum foil, with a length of about 500 nm and a thickness of 10 nm, and the nanosheets are scattered on the surface of the molybdenum foil, which is uneven. Figures 1(b) and 1(e) are scanning electron microscope images (SEM) with 0.3 mmol S added to the synthesis. Here we can see that the material morphology is dense two-dimensional nanosheets, which are petal-shaped. With the increase of the amount of S added, the number of  $\text{MoS}_2$  nanosheets increased, and the scattered uneven nanosheets became dense after the increase in number, and formed a petal shape vertically. Fig. 1(c) and Fig. 1(f) are scanning electron microscope (SEM) images with 0.6 mmol S added during synthesis, and it can be seen from the SEM images that there are more flake  $\text{MoS}_2$  nanosheets on the surface of molybdenum foil, and the size of the nanosheets is consistent with the previous two. As the amount of S added continued, the number of  $\text{MoS}_2$  nanosheets continued, but the structure changed from dense petals to loose arrangement. We study the phase of nanosheets by powder X-ray diffraction (XRD). In order to avoid interference from the Mo foil, the Mo foil is passed through ultrasonication and the peeled samples are tested. As shown in Figure 1 (g), the characteristic peaks were detected at  $14.1^\circ$ ,  $33.1^\circ$ ,  $39.8^\circ$ , and  $58.7^\circ$  in the XRD patterns of all samples, corresponding to the (002), (101), (103), and (110) planes of 2H- $\text{MoS}_2$  (JCPDS 37-1492), respectively. The XRD characteristic peak distribution of the samples was basically consistent with that of 2H- $\text{MoS}_2$  (JCPDS 37-1492), indicating that we had successfully grown  $\text{MoS}_2$  nanosheets on the surface of molybdenum foil.

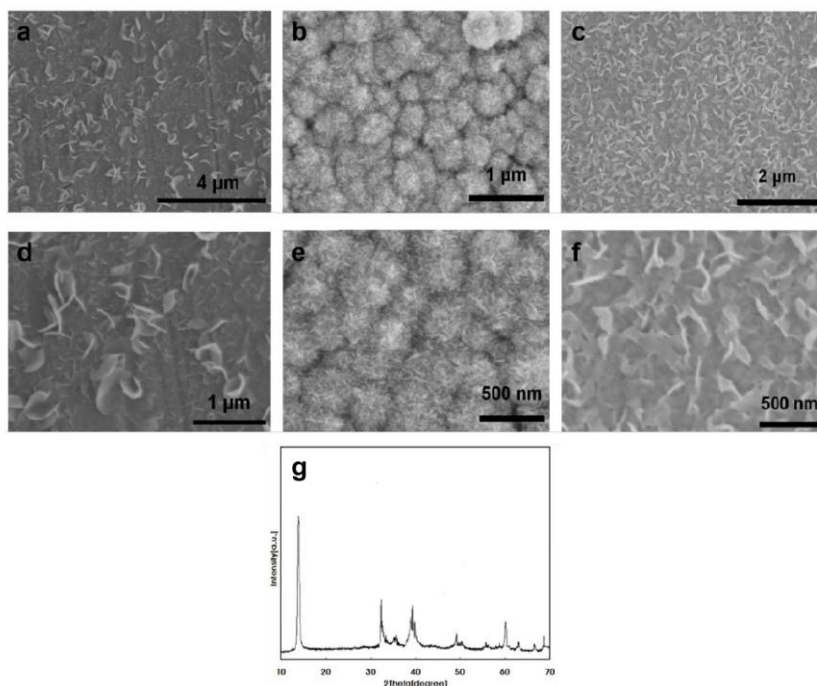


Figure 1: SEM image of MoS<sub>2</sub>@Mo, (a, d) MoS<sub>2</sub>@Mo-1 SEM image with 0.1 mmol S, (b, e) MoS<sub>2</sub>@Mo-3 SEM image with 0.3 mmol S, (c, f) MoS<sub>2</sub>@Mo-6 SEM image with 0.6 mmol S, (g) XRD image of the material from the surface peeling of Mo foil

### 3.2 Catalytic HER performance of MoS<sub>2</sub>@Mo nanomaterials over a wide pH range

To compare the HER performance of the above-mentioned MoS<sub>2</sub>@Mo nanomaterials synthesized with different amounts of S, we first compared the catalytic HER activity of MoS<sub>2</sub>@Mo-1, MoS<sub>2</sub>@Mo-3, and MoS<sub>2</sub>@Mo-6 in 1 M KOH (pH = 14). The HER activity of these samples in an alkaline environment was assessed by comparing the polarization curves obtained by linear scanning voltammetry (LSV) testing. Considering that the obtained current density may not reflect the actual catalytic HER performance of the sample due to the presence of ohmic resistance, iR compensation was performed for all polarization curves prior to analysis [20].

As can be seen from Figure 2(a), Mo foil and MoS<sub>2</sub>@Mo-1 show poor HER activity in the alkaline environment of 1 M KOH solution. The HER activity of the MoS<sub>2</sub>@Mo was significantly increased after the growth of MoS<sub>2</sub> nanosheets on the surface of Mo foil. Specifically, the Mo foil electrode has an overpotential of 378 mV at 10 mA•cm<sup>-2</sup> and 271 mV at 10 mA•cm<sup>-2</sup> for the MoS<sub>2</sub>@Mo-1 electrode. This suggests that our strategy of growing MoS<sub>2</sub> nanosheets on the surface of Mo foil can enhance the HER activity of the material in an alkaline environment. The electrode made of MoS<sub>2</sub>@Mo-3 with 0.3 mmol S had an overpotential of 40 mV at 10 mA•cm<sup>-2</sup>. The electrode made of MoS<sub>2</sub>@Mo-6 with 0.6 mmol S has an overpotential of 151 mV at 10 mA•cm<sup>-2</sup>. It can be seen that the catalytic HER activity of MoS<sub>2</sub>@Mo does not increase linearly with the increase of the amount of S added: when the amount of S added increases from 0.1 mmol to 0.3 mmol, the MoS<sub>2</sub>@Mo catalytic HER activity increases. When the amount of S was increased from 0.3 mmol to 0.6 mmol, the activity of MoS<sub>2</sub>@Mo catalytic HER decreased compared with the previous one. Because the structure of MoS<sub>2</sub> synthesized is a homogeneous and non-aggregated nanosheet, the catalytic active site of the MoS<sub>2</sub> nanosheet is concentrated at the edge of the sheet, while the base surface that occupies the main component is inert and the conductivity of MoS<sub>2</sub> is poor. Therefore, the structure of MoS<sub>2</sub> has a great influence on its HER catalytic performance. There are two main modes of MoS<sub>2</sub> nanosheets: horizontal and vertical growth. Compared with horizontal growth, vertically grown MoS<sub>2</sub> has more full exposure to the active edge and can have more adequate contact with the electrolyte. Due to the large number of exposed marginal active sites, the exchange current density of this MoS<sub>2</sub> as a hydrogen evolution catalyst is about 10 times that of ordinary layered MoS<sub>2</sub><sup>[21][22]</sup>. In the MoS<sub>2</sub>@Mo-1 we synthesized this time, the number of MoS<sub>2</sub> nanosheets was small, and they lacked support between each other, and they were scattered on the Mo foil, and a large number of MoS<sub>2</sub> nanosheets could not fully contact the electrolyte due to the horizontal growth. Therefore, the catalytic activity of MoS<sub>2</sub>@Mo-1 is the lowest of the three. With the increase of the addition of S, the number of MoS<sub>2</sub> nanosheets increased, which supported each other to

form a petal-like structure<sup>[23]</sup>. Combined with Fig. 1(b,e), we can see that most of the MoS<sub>2</sub> nanosheets in MoS<sub>2</sub>@Mo-3 are growing vertically, and this structure exposes more catalytic active sites at the edge of the lamellar, which greatly improves the catalytic activity of the material. Therefore MoS<sub>2</sub>@Mo-3 has the best HER catalytic activity of the three. However, as the addition of S continued to increase, the number of MoS<sub>2</sub> nanosheets continued to increase, and too many MoS<sub>2</sub> nanosheets squeezed each other, destroying the original petal-like structure, and the vertically growing nanosheets collapsed into horizontal growth, resulting in a decrease in the catalytic activity of the material. Therefore MoS<sub>2</sub>@Mo-6 has a reduced HER catalytic activity, which is not as good as MoS<sub>2</sub>@Mo-3. We further investigated the catalytic performance of MoS<sub>2</sub>@Mo in acidic media. Fig. 2(b) shows that the overpotential of the Mo foil electrode is 378 mV at 10 mA•cm<sup>-2</sup>, the overpotential of the MoS<sub>2</sub>@Mo-1 electrode is 213.5 mV at 10 mA•cm<sup>-2</sup>, the overpotential of the MoS<sub>2</sub>@Mo-3 electrode is 142.5 mV at 10 mA•cm<sup>-2</sup>, and the overpotential of the MoS<sub>2</sub>@Mo-6 electrode is 169.6 mV at 10 mA•cm<sup>-2</sup>. The catalytic HER performance of the same material in alkaline environments is better than that of catalytic HER in acidic environments.

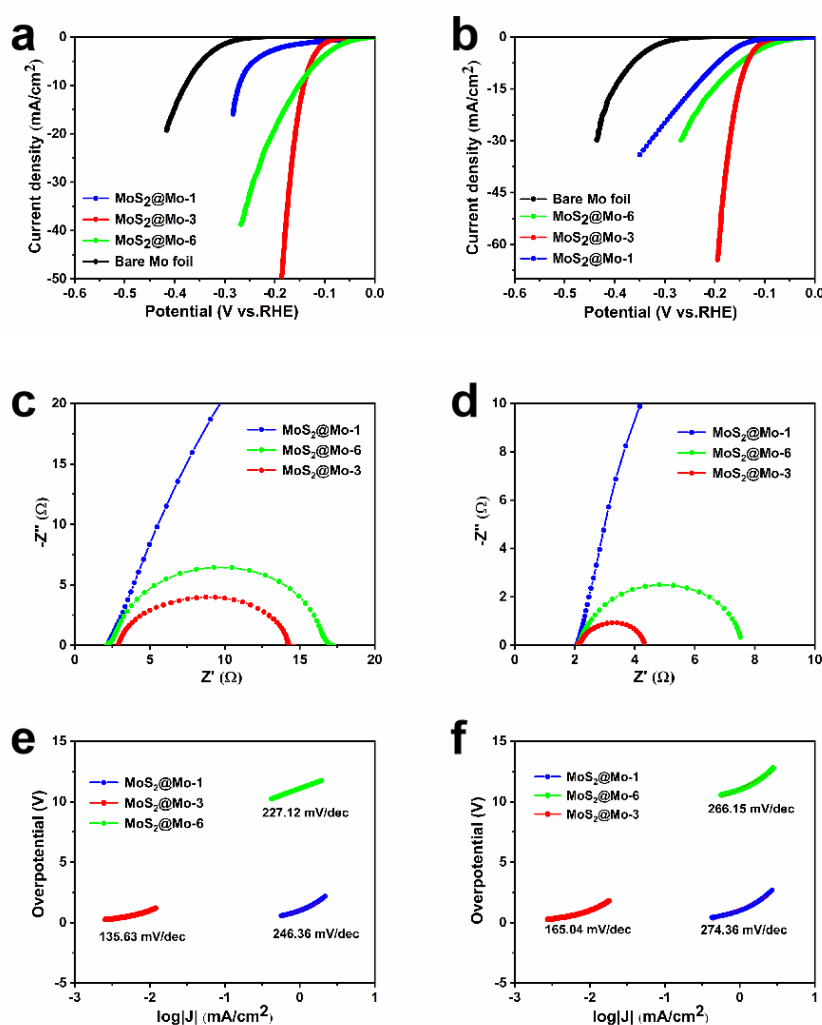


Figure 2(a) Polarization curves of MoS<sub>2</sub>@Mo-1, MoS<sub>2</sub>@Mo-3, MoS<sub>2</sub>@Mo-6 and bare Mo foil in 1 M KOH solution, Figure 2(b) Polarization curves of MoS<sub>2</sub>@Mo-1, MoS<sub>2</sub>@Mo-3, MoS<sub>2</sub>@Mo-6 and bare Mo foil in 0.5 M H<sub>2</sub>SO<sub>4</sub> solution, and Figure 2(c) Nyquist plot of MoS<sub>2</sub>@Mo-1, MoS<sub>2</sub>@Mo-3, MoS<sub>2</sub>@Mo-6 in 1 M KOH solution, Figure 2(d) Nyquist plot of MoS<sub>2</sub>@Mo-1, MoS<sub>2</sub>@Mo-3, MoS<sub>2</sub>@Mo-6 in 0.5 M H<sub>2</sub>SO<sub>4</sub> solution, Figure 2(e) Tafel plot of MoS<sub>2</sub>@Mo-1, MoS<sub>2</sub>@Mo-3, MoS<sub>2</sub>@Mo-6 in 1 M KOH solution, Figure 2(f) Tafel plot of MoS<sub>2</sub>@Mo-1, MoS<sub>2</sub>@Mo-3, MoS<sub>2</sub>@Mo-6 in 0.5 M H<sub>2</sub>SO<sub>4</sub> solution.

Figure 2: Catalytic HER performance of MoS<sub>2</sub>@Mo nanomaterials.

Electrochemical impedance spectroscopy (EIS) studies the preparation of electrocatalysts at the electrode/electrolyte boundary at open-circuit voltages. The HER dynamics at the surface, which can be fitted by an equivalent circuit<sup>[24][19]</sup>, can derive their R<sub>ct</sub>, which in turn reflects their charge transport

efficiency<sup>[25]</sup>. Figure 2(c) shows the EIS profile of MoS<sub>2</sub>@Mo-1, MoS<sub>2</sub>@Mo-3, MoS<sub>2</sub>@Mo-6 in 1 M KOH solution, with charge transfer resistance (R<sub>ct</sub>) of 15, 10, and 64 Ω for MoS<sub>2</sub>@Mo-1, MoS<sub>2</sub>@Mo-3, MoS<sub>2</sub>@Mo-6, respectively. The charge transfer resistance (R<sub>ct</sub>) of MoS<sub>2</sub>@Mo-1, MoS<sub>2</sub>@Mo-3, MoS<sub>2</sub>@Mo-6 in 0.5 M H<sub>2</sub>SO<sub>4</sub> solution was 6, 2.2, and 51 Ω, respectively. By comparison, we can see that the RCT value of MoS<sub>2</sub>@Mo-3 is lower than that of other samples, indicating that it has better charge transport kinetics. The results show that the petal-like structure is more conducive to the transfer of charge during hydrogen evolution than the scattered vertical and horizontal growth structures, that is, the design of the petal-like structure can effectively improve the conductivity of MoS<sub>2</sub>. The results show that MoS<sub>2</sub>@Mo-3 has the highest electronic conductivity and a faster transfer rate of charge between catalyst/electrolyte, which is conducive to electrocatalytic reactions. Combined with Fig. 2(c,d), we can observe that the effect of this petal-like structure in improving the conductivity of MoS<sub>2</sub> nanosheets is reflected in both acid and alkali solutions.

To investigate the kinetic mechanism and rate-determining steps of the catalyst in HER, we evaluated the Tafel slope (where b is the Tafel slope, η is the overpotential, and j is the current density) according to the polarization curve with the Tafel equation  $\eta = a + b \log(j)$ <sup>[26][27]</sup>. It is well known that the HER method consists of two main steps, including hydrogen adsorption and desorption. In alkaline solutions, hydrogen adsorption occurs in the Volmer reaction ( $H_2O + * + e^- \rightarrow H^* + OH^-$ , where \* is the active site and H\* is the adsorbed hydrogen)<sup>[28]</sup>. The H<sub>2</sub> desorption step consists of either the Heyrovsky reaction ( $H^* + H_2O + e^- \rightarrow H_2 + * + OH^-$ ) or the Tafel reaction ( $H^* + H^* \rightarrow H_2 + 2*$ ). Therefore, the reaction path of HER is basically divided into three reaction mechanisms: the first is the Volmer-Tafel mechanism, which has a Tafel slope range of 0~38 mV·dec<sup>-1</sup>, the second is the Volmer-Heyrovsky mechanism, which has a Tafel slope range of 38~116 mV·dec<sup>-1</sup>, and the third is the Volmer mechanism, which has a Tafel slope range of >116 mV·dec<sup>-1</sup>. Figure 2(e) shows that the Tafel slope is 246.36 mV/dec for MoS<sub>2</sub>@Mo-1, 135.63 mV/dec for MoS<sub>2</sub>@Mo-3, and 227.12 mV/dec for MoS<sub>2</sub>@Mo-6. It is suggested that the HER process of three materials in the alkaline environment of 1 M KOH may be a Volme mechanism [22]. In addition, a smaller Tafel slope value means that the HER rate increases more quickly with a modest increase in overpotential, so an ideal HER catalyst should have a small Tafel slope value. The floral MoS<sub>2</sub>@Mo-3 has a small Tafel slope value, indicating that its catalytic hydrogen evolution reaction performance is better than that of the nanosheet-arranged MoS<sub>2</sub>@Mo-1 (246.36 mV/dec) and MoS<sub>2</sub>@Mo-6 (227.12 mV/dec). Figure 2(f) shows that the Tafel slope values for MoS<sub>2</sub>@Mo-1, MoS<sub>2</sub>@Mo-3, and MoS<sub>2</sub>@Mo-6 are 274.36 mV/dec, 165.04 mV/dec, and 266.15 mV/dec, respectively. The Tafel slope value of MoS<sub>2</sub>@Mo-3 is still the smallest. From the perspective of tafel slope, the catalytic performance of MoS<sub>2</sub>@Mo-3 is still the best.

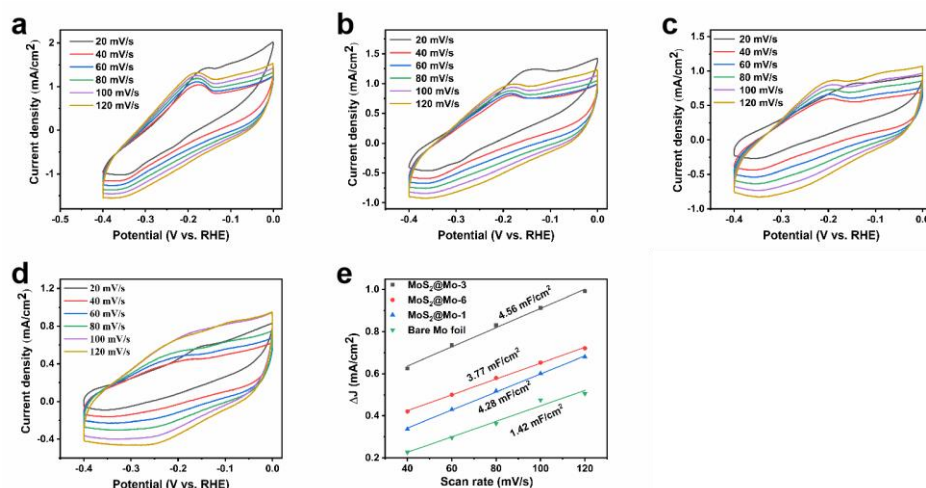


Figure 3 (a): CV plots of different scan rates of Bare Mo foil under alkaline conditions; Figure 3(b,c,d) CV plots of different scan rates for MoS<sub>2</sub>@Mo-1, MoS<sub>2</sub>@Mo-3, MoS<sub>2</sub>@Mo-6 under alkaline conditions; Figure 3(e) Cdl plots of MoS<sub>2</sub>@Mo-1, MoS<sub>2</sub>@Mo-3, MoS<sub>2</sub>@Mo-6 and Bare Mo foil under alkaline conditions.

In order to understand the source of the performance improvement of MoS<sub>2</sub>@Mo-3, its electrochemical activity area (ECSA) and specific activity were studied, and the results obtained were compared with Mo foil, MoS<sub>2</sub>@Mo-1 and MoS<sub>2</sub>@Mo-6. Since the electric double-layer capacitance (Cdl) has a linear relationship with the electrochemically active surface area (ECSA)<sup>[29][30]</sup>, i.e., the ECSA is twice that of (Cdl), the electrochemically active surface area can be calculated by Cdl. The

electric double-layer capacitance value (Cdl) can be used to compare the size of the electrochemical active area, and the Cdl value is generally calculated by cyclic voltammetry<sup>[31]</sup>. We calculated the forward and reverse sweep current difference between the CV test of MoS<sub>2</sub>@Mo-3 and Mo foil, MoS<sub>2</sub>@Mo-1, and MoS<sub>2</sub>@Mo-6 at different scan rates under alkaline conditions, and found that the current difference was linearly related to the scan rate, as shown in Figure 3(e), and the slope of the linear relationship was the CDL of the catalytic material. As shown in Figure 3(e) above, the Cdl value of MoS<sub>2</sub>@Mo-3 is 4.56 mF/cm<sup>2</sup> under alkaline conditions, 4.28 mF/cm<sup>2</sup> for MoS<sub>2</sub>@Mo-1, 3.77 mF/cm<sup>2</sup> for MoS<sub>2</sub>@Mo-6, and 1.42 mF/cm<sup>2</sup> for pure molybdenum foil. The ECSA of MoS<sub>2</sub>@Mo-3 was 1.2 times that of MoS<sub>2</sub>@Mo-6 and 1.3 times that of MoS<sub>2</sub>@Mo-1. The results suggest that the design of the petal-like structure of MoS<sub>2</sub>@Mo-3 increases the ECSA of MoS<sub>2</sub> and creates more HER active sites. The electric double-layer capacitance of the synthesized MoS<sub>2</sub>@Mo nanotube array material increases significantly, indicating that the electrochemically active area of the material increases<sup>[32][33]</sup>. Therefore, the nanotube array structure of the synthesized product effectively increases the electrochemical active area of the material, which is conducive to increasing the number of active sites of the catalyst and improving the HER performance of the material.

#### 4. Conclusion

In this paper, flake MoS<sub>2</sub> nanomaterials were successfully prepared on the surface of molybdenum foil by hydrothermal method, and the prepared MoS<sub>2</sub> can be directly used as a cathode material for electrolysis of water and hydrogen evolution because the prepared MoS<sub>2</sub> is directly grown on molybdenum foil. The good conductivity of molybdenum foil enhances the electron transport rate of the product, and the petal-like MoS<sub>2</sub> nanosheet structure also exposes more active sites, increases the electrochemical active area, and the electron conductivity is higher, and the charge transfer rate between the catalyst/electrolyte is faster and can contact the electrolyte more closely, thereby improving the catalytic activity of the material. A series of electrochemical tests have shown that the synthesized MoS<sub>2</sub>@Mo nanomaterials exhibit excellent electrocatalytic HER properties in both acidic and alkaline environments, which provides a new idea for the design of metal-based nanomaterials in the future.

#### Acknowledgement

Fund project: wzyzr202418, wzyzr202416.

#### References

- [1] Lu SQ, Zhuang ZB. *Electrocatalysts for hydrogen oxidation and evolution reactions*. *Sci China Mater*, 2016, 59: 217-238.
- [2] Morales-Guio CG, Stern LA, Hu XL. *Nanostructured hydrotreating catalysts for electrochemical hydrogen evolution*. *Chem Soc Rev*, 2014, 43: 6555-6569.
- [3] Yuan P, Chao Z, Yan L, et al. *Electrocatalyst engineering and structure–activity relationship in hydrogen evolution reaction: From nanostructures to single atoms*. *Sci China Mater*, 2020, 63(6):921-948.
- [4] Huang YZ, Liu L. *Recent progress in atomic layer deposition of molybdenum disulfide: A mini review*. *Sci China Mater*, 2019, 62: 913-924.
- [5] Eftelthari A. *Molybdenum diselenide (MoSe<sub>2</sub>) for energy storage, catalysis, and optoelectronics*. *Appl Mater Today*, 2017, 8: 1-17.
- [6] Hong M, Shi JP, Huan YH, et al. *Microscopic insights into the catalytic mechanisms of monolayer MoS<sub>2</sub> and its heterostructures in hydrogen evolution reaction*. *Nano Res*, 2019, 12: 2140-2149.
- [7] Chhowalla M, Shin HS, Eda G, et al. *The chemistry of two-dimensional layered transition metal dichalcogenide nanosheets*. *Nat Chem*, 2013, 5: 263-275.
- [8] Wang PP, Sun HY, Ji YJ, et al. *Three-dimensional assembly of single-layered MoS<sub>2</sub>*. *Adv Mater*, 2014, 26: 964-969.
- [9] Wang H, Xiao X, Liu SY, et al. *Structural and electronic optimization of MoS<sub>2</sub> edges for hydrogen evolution*. *J Am Chem Soc*, 2019, 141: 18578-18584.
- [10] Zhang, X., Shao, J., Huang, W. et al. *Three dimensional carbon substrate materials for electrolysis of water*. *Sci. China Mater*. 61, 1143–1153 (2018).<https://doi.org/10.1007/s40843-018-9295-8>
- [11] Deng SJ, Zhong Y, Zeng YX, et al. *Directional construction of vertical nitrogen-doped 1T-2H*

MoSe<sub>2</sub>/graphene shell/core nanoflake arrays for efficient hydrogen evolution reaction. *Adv Mater*, 2017, 29: 1700748.

[12] Qu B, Yu XB, Chen YJ, et al. Ultrathin MoSe<sub>2</sub> nanosheets decorated on carbon fiber cloth as binder-free and high-performance electrocatalyst for hydrogen evolution. *ACS Appl Mater Interfaces*, 2015, 7: 14170-14175.

[13] Sun KA, Zeng LY, Liu SH, et al. Design of basal plane active MoS<sub>2</sub> through one-step nitrogen and phosphorus Co-doping as an efficient pH-universal electrocatalyst for hydrogen evolution. *Nano Energy*, 2019, 58: 862-869.

[14] Yan Y, Xia BY, Li N, et al. Vertically oriented MoS<sub>2</sub> and WS<sub>2</sub> nanosheets directly grown on carbon cloth as efficient and stable 3-dimensional hydrogen-evolving cathodes. *J Mater Chem A*, 2015, 3: 131-135.

[15] Xie JF, Qu HC, Xin JP, et al. Defect-rich MoS<sub>2</sub> nanowall catalyst for efficient hydrogen evolution reaction. *Nano Res*, 2017, 10: 1178-1188.

[16] Khan AA, Labbe JC. Aluminium nitride-molybdenum ceramic matrix composites: Characterization of ceramic-metal interface. *J Eur Ceram Soc*, 1996, 16: 739-744.

[17] Xu Y, Zheng C, Wang SB, et al. 3D arrays of molybdenum sulphide nanosheets on Mo meshes: Efficient electrocatalysts for hydrogen evolution reaction. *Electrochim Acta*, 2015, 174: 653-659.

[18] Shen BW, Che YX, Luo YJ, et al. *Inorganic chemistry series: Titanium group vanadium group chromium group*. Beijing: Science Press, 1998: 457.

[19] Lu ZY, Zhang HC, Zhu W, et al. In situ fabrication of porous MoS<sub>2</sub> thin-films as high-performance catalysts for electrochemical hydrogen evolution. *Chem Commun*, 2013, 49: 7516-7518.

[20] Pu ZH, Liu Q, Asiri AM, et al. 3D macroporous MoS<sub>2</sub> thin film: In situ hydrothermal preparation and application as a highly active hydrogen evolution electrocatalyst at all pH values. *Electrochim Acta*, 2015, 168: 133-138.

[21] Liu H, Liu BH, Guo H, et al. N-doped C-encapsulated scale-like yolk-shell frame assembled by expanded planes few-layer MoSe<sub>2</sub> for enhanced performance in sodium-ion batteries. *Nano Energy*, 2018, 51: 639-648.

[22] Wang WZ, Xu YF, Liu Q, et al. One-dimensional hierarchical structured MoS<sub>2</sub> with an ordered stacking of nanosheets: A facile template-free hydrothermal synthesis strategy and application as an efficient hydrogen evolution electrocatalyst. *CrystEngComm*, 2017, 19: 218-223.

[23] Wang HT, Kong DS, Johanes P, et al. MoSe<sub>2</sub> and WSe<sub>2</sub> nanofilms with vertically aligned molecular layers on curved and rough surfaces. *Nano Lett*, 2013, 13:3426-3433.

[24] Tongay S, Zhou J, Ataca C, et al. Thermally driven crossover from indirect toward direct bandgap in 2D semiconductors: MoSe<sub>2</sub> versus MoS<sub>2</sub>. *Nano Lett*, 2012, 12: 5576-5580.

[25] Lu X, Utama MIB, Lin JH, et al. Large-area synthesis of monolayer and few-layer MoSe<sub>2</sub> films on SiO<sub>2</sub> substrates. *Nano Lett*, 2014, 14: 2419-2425.

[26] Shaw JC, Zhou HL, Chen Y, et al. Chemical vapor deposition growth of monolayer MoSe<sub>2</sub> nanosheets. *Nano Res*, 2014, 7: 511-517.

[27] Roberge PR, Beaudoin R. Evaluation of charge transfer resistance by geometrical extrapolation of the centre of semicircular impedance diagrams. *J Appl Electrochem*, 1988, 18: 38-42.

[28] Wang H, Sun C, Cao YJ, et al. Molybdenum carbide nanoparticles embedded in nitrogen-doped porous carbon nanofibers as a dual catalyst for hydrogen evolution and oxygen reduction reactions. *Carbon*, 2017, 114: 628-634.

[29] QI K, YU S S, WANG Q Y, et al. Decoration of the inert basal plane of defectrich MoS<sub>2</sub> with Pd atoms for achieving Pt-similar HER activity. *Journal of Materials Chemistry A*, 2016, 4: 4025-4031.

[30] BOLAR S, SHIT S, MURMU N C, et al. Activation strategy of MoS<sub>2</sub> as HER electrocatalyst through doping-induced lattice strain, band gap engineering, and active crystal plane design. *ACS Applied Materials & Interfaces*, 2021, 13: 765-780.

[31] SHI Y, ZHOU Y, YANG D R, et al. Energy level engineering of MoS<sub>2</sub> by transition-metal doping for accelerating hydrogen evolution reaction. *Journal of the American Chemical Society*, 2017, 139: 15479-15485.

[32] KONG D S, WANG H T, CHA J J, et al. Synthesis of MoS<sub>2</sub> and MoSe<sub>2</sub> films with vertically aligned layers. *Nano Letters*, 2013, 13: 1341-1347.

[33] JUNG Y W, SHEN J, LIU Y H, et al. Metal seed layer thickness-induced transition from vertical to horizontal growth of MoS<sub>2</sub> and WS<sub>2</sub>. *Nano Letters*, 2014, 14: 6842-6849.